



Correlated edge overlaps in multiplex networks.

Baxter, GJ; Bianconi, G; da Costa, RA; Dorogovtsev, SN; Mendes, JF

“Original publication is available at

<http://journals.aps.org/pre/abstract/10.1103/PhysRevE.94.012303>”

For additional information about this publication click this link.

<http://qmro.qmul.ac.uk/xmlui/handle/123456789/13915>

Information about this research object was correct at the time of download; we occasionally make corrections to records, please therefore check the published record when citing. For more information contact scholarlycommunications@qmul.ac.uk

Correlated Edge Overlaps in Multiplex Networks

Gareth J. Baxter,¹ Ginestra Bianconi,² Rui A. da Costa,¹ Sergey N. Dorogovtsev,^{1,3} and José F. F. Mendes¹

¹*Department of Physics & I3N, University of Aveiro, 3810-193 Aveiro, Portugal*

²*School of Mathematical Sciences, Queen Mary University of London, London, E1 4NS, United Kingdom*

³*A. F. Ioffe Physico-Technical Institute, 194021 St. Petersburg, Russia*

We develop the theory of sparse multiplex networks with partially overlapping links based on their local tree-likeness. This theory enables us to find the giant mutually connected component in a two-layer multiplex network with arbitrary correlations between connections of different types. We find that correlations between the overlapping and non-overlapping links markedly change the phase diagram of the system, leading to multiple hybrid phase transitions. For assortative correlations we observe recurrent hybrid phase transitions.

PACS numbers: 89.75.Fb,64.60.aq,05.70.Fh,64.60.ah

I. INTRODUCTION

Most real networks are not independent but must be treated as sets of interdependent networks (layers) [1, 2]. One of the simplest models of complexes of this kind is a multiplex network. Each layer contains the same nodes, but connected by links specific to that layer. In other words, a multiplex network is a graph with nodes of one type connected by links of multiple types (colors). A natural generalization of percolation on a single network—giant connected component—to multiplex networks is the giant mutually connected component (mutual component). It is defined by the rule that for every pair of nodes in the mutual component, there must be a path between them in each layer (which remains within the mutual component). Under this definition of percolation, a discontinuous hybrid transition occurs in sparse multiplex networks [3, 4].

In real networks, physical or other constraints mean that edges from different layers are likely to be co-located. To cater for this possibility, the multiplex concept has been further generalised to consider the case that two nodes may be connected by more than one color of edge [5–8] with nonvanishing probability. The simplest example is a two-layer multiplex network. In this type of network two nodes i and j can be connected in three different ways: by an edge only in layer 1, and edge only on layer 2, or by edges in both layers, which we will call an overlapping edge.

A message passing approach was proposed in Ref. [5] to characterize the giant mutually connected component of multiplex networks with overlap of the links, but it was later found [7] that the algorithm characterizes instead a distinct directed percolation problem for multiplex networks. Another recent work has proposed a more complex iterative scheme requiring an intermediate remapping of the network [6]. This model agrees with numerical simulations of the mutually connected component of multiplex networks with overlap [7].

Here we consider the more general problem in a two layered multiplex network, in which we allow arbitrary correlations between the degrees with respect to the three

types of connection. We exploit the locally tree-like structure of infinite sparse random networks to directly write strict self-consistency equations which allow the solution of the problem.

Note the following difference from the problem without overlapped edges. A cluster of nodes connected by overlapped edges belongs to the giant mutual component if at least one node of the cluster is connected to this component in each layer, even if these nodes are different. In Ref. [6] the calculation was done by compressing the overlapped clusters into “supernodes”, and then considering non-overlapping multiplex percolation on the resulting network. This requires a rather arduous process of finding both mass and degree distributions for these supernodes, and then incorporating a separate generating function for each size of overlapped clusters. In Refs. [6, 7] the calculation is done under the assumption overlapped and non-overlapped degrees are uncorrelated. Consideration of degree correlations using this method, while in principle possible, would require modification of a significant step in this calculation. Here we show that the calculation can in fact be done straightforwardly in the usual self-consistency equation fashion, making for a much simpler and more direct calculation. Furthermore, no assumptions about correlations need to be made, so arbitrary correlations among the three connection types can be examined without modification of the method.

We are therefore able to confirm the results of Ref. [6], but using a far simpler calculation, and then generalize them to more complex and interesting situations. We use our equations to examine the effect of correlations between overlapped and non-overlapped edge placement. We find that correlations qualitatively change the phase diagram, with the giant mutually connected component emerging through consecutive hybrid transitions. Remarkably, in the particular case of assortative correlations one of these transitions can be recurrent.

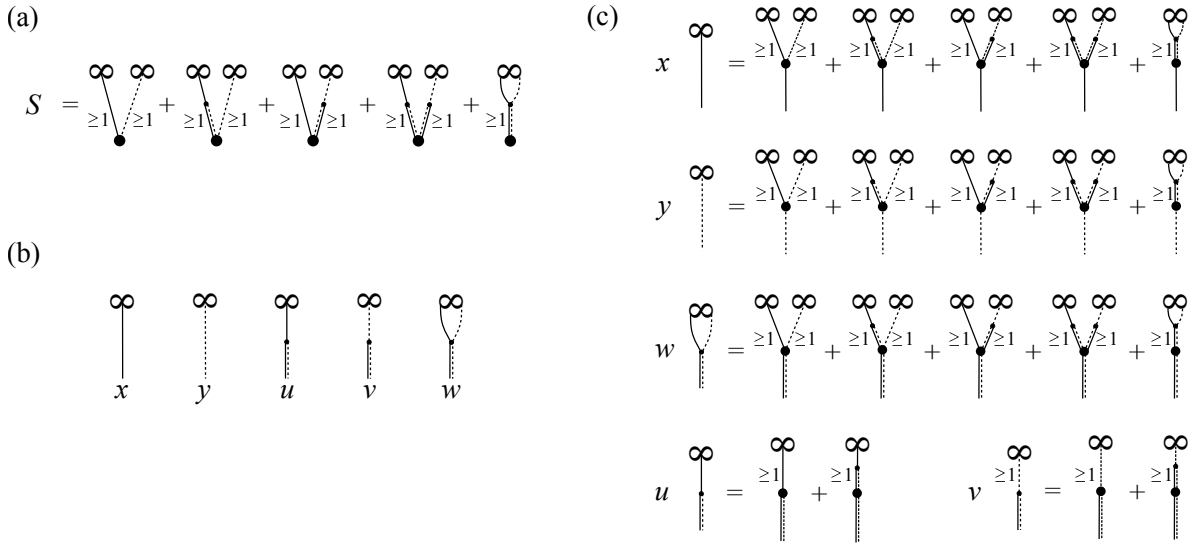


FIG. 1. (a) Graphical representation of the expression for the size of the mutual component S , Eq. (1), and (c) of the equations for the five probabilities, Eq. (2), using notations (b) for five probabilities.

II. MODEL AND EQUATIONS

We consider a generalized configuration model for sparse multiplex networks in the infinite size limit, in which each node has three degrees q_1 , q_2 , \tilde{q} , being, respectively, the number of connections only in layer 1, only in layer 2, and the number of overlapping connections. The network is then defined by the joint degree distribution $P(q_1, q_2, \tilde{q})$. If a node is connected to the gi-

ant mutually connected component in both layers, then it too belongs to the giant mutually connected component. A single overlapping edge is sufficient to provide this connection. As noted above, one must therefore carefully consider overlapped clusters when making percolation calculations. Alternatively at least one single edge of each type is needed to provide this connection. These considerations lead to the following expression for the relative size S of the giant mutually connected component, represented graphically in Fig. 1(a):

$$\begin{aligned}
 S &= \sum_{q_1, q_2, \tilde{q}} P(q_1, q_2, \tilde{q}) \left\{ [1 - (1-x)^{q_1}] [1 - (1-y)^{q_2}] (1-u-v-w)^{\tilde{q}} + [1 - (1-x)^{q_1}] [(1-u-w)^{\tilde{q}} - (1-u-v-w)^{\tilde{q}}] \right. \\
 &\quad \left. + [1 - (1-y)^{q_2}] [(1-v-w)^{\tilde{q}} - (1-u-v-w)^{\tilde{q}}] + [(1-w)^{\tilde{q}} - (1-w-u)^{\tilde{q}} - (1-w-v)^{\tilde{q}} + (1-w-u-v)^{\tilde{q}}] + [1 - (1-w)^{\tilde{q}}] \right\} \\
 &= 1 - \sum_{q_1, q_2, \tilde{q}} P(q_1, q_2, \tilde{q}) [(1-x)^{q_1} (1-w-u)^{\tilde{q}} + (1-y)^{q_2} (1-w-v)^{\tilde{q}} - (1-x)^{q_1} (1-y)^{q_2} (1-w-u-v)^{\tilde{q}}]. \quad (1)
 \end{aligned}$$

We define x to be the probability that, on following an arbitrary edge in layer 1, we encounter a node belonging to the giant mutual component, and y as the corresponding probability on following an edge in layer 2. For overlapping edges, we must consider three probabilities. First, u is the probability that, on following an overlapped edge, we encounter a node with at least one other connection to the giant mutual component by an edge in layer 1, and v

is the probability that the node reached has a connection to the giant mutual component in layer 2. Finally w is the probability that if we follow an arbitrary overlapped edge we reach a node which has connections to the giant mutual component in both layer 1 and layer 2 (not overlapped). These probabilities are represented graphically in Fig. 1(b). They obey the following self-consistency equations, represented graphically in Fig. 1(c):

$$\begin{aligned}
x &= 1 - \sum_{q_1, q_2, \tilde{q}} \frac{q_1}{\langle q_1 \rangle} P(q_1, q_2, \tilde{q}) [(1-x)^{q_1-1} (1-u-w)^{\tilde{q}} + (1-y)^{q_2} (1-v-w)^{\tilde{q}} - (1-x)^{q_1-1} (1-y)^{q_2} (1-u-v-w)^{\tilde{q}}], \\
y &= 1 - \sum_{q_1, q_2, \tilde{q}} \frac{q_2}{\langle q_2 \rangle} P(q_1, q_2, \tilde{q}) [(1-x)^{q_1} (1-u-w)^{\tilde{q}} + (1-y)^{q_2-1} (1-v-w)^{\tilde{q}} - (1-x)^{q_1} (1-y)^{q_2-1} (1-u-v-w)^{\tilde{q}}], \\
u &= \sum_{q_1, q_2, \tilde{q}} \frac{\tilde{q}}{\langle \tilde{q} \rangle} P(q_1, q_2, \tilde{q}) (1-y)^{q_2} [(1-v-w)^{\tilde{q}-1} - (1-x)^{q_1} (1-u-v-w)^{\tilde{q}-1}], \\
v &= \sum_{q_1, q_2, \tilde{q}} \frac{\tilde{q}}{\langle \tilde{q} \rangle} P(q_1, q_2, \tilde{q}) (1-x)^{q_1} [(1-u-w)^{\tilde{q}-1} - (1-y)^{q_2} (1-u-v-w)^{\tilde{q}-1}], \\
w &= 1 - \sum_{q_1, q_2, \tilde{q}} \frac{\tilde{q}}{\langle \tilde{q} \rangle} P(q_1, q_2, \tilde{q}) [(1-x)^{q_1} (1-u-w)^{\tilde{q}-1} + (1-y)^{q_2} (1-v-w)^{\tilde{q}-1} - (1-x)^{q_1} (1-y)^{q_2} (1-u-v-w)^{\tilde{q}-1}]. \quad (2)
\end{aligned}$$

Solution of Eqs. (2) and then substitution into Eq. (1) allows one to find the size of the giant mutually connected component for networks with arbitrary intra- and inter-layer degree correlations.

If the joint degree distribution is symmetric with respect to the two layers, i.e. $P(q, q', \tilde{q}) = P(q', q, \tilde{q})$, this system is reduced to three equations for $x = y$, $u = v$, and w . We now demonstrate the solution of the system of Eqs. (2) in several representative cases.

III. UNCORRELATED CASE

We first show that previous results for the uncorrelated case can straightforwardly be reproduced by our method. If correlations are absent, and $P(q_1, q_2, \tilde{q}) = \mathcal{P}(q_1, c) \mathcal{P}(q_2, c) \mathcal{P}(\tilde{q}, \tilde{c})$, where $\mathcal{P}(q, c)$ is a Poisson distribution with mean c , then $S = x = y = w$, $u = v$, and we arrive at a system of two equations:

$$\begin{aligned}
x &= 1 - e^{-cx} e^{-\tilde{c}(x+u)} [2 - e^{-(cx+\tilde{c}u)}], \\
u &= e^{-cx} e^{-\tilde{c}(x+u)} [1 - e^{-(cx+\tilde{c}u)}]. \quad (3)
\end{aligned}$$

The solution of this system readily gives $S(c, \tilde{c})$, the size of the giant mutually connected component as a function of the mean intra-layer degree c and inter-layer degree \tilde{c} . The giant mutual component appears with a discontinuous hybrid phase transition. The phase diagram is shown in Fig. 2(a). These results agrees perfectly with the theoretical and numerical results presented in [6, 7].

IV. CORRELATIONS BETWEEN INTER- AND INTRALAYER DEGREES

An advantage of our method is that these results may be extended to consider degree correlations without much more difficulty. We explore the effect of degree correlations by considering random networks where the average number of overlapping links $\tilde{c} = f(q_1 + q_2)$ is a function

of the number of single edges $q_1 + q_2$ for a given node, thus:

$$P(q_1, q_2, \tilde{q}) = \mathcal{P}(q_1, c) \mathcal{P}(q_2, c) \mathcal{P}[\tilde{q}, f(q_1 + q_2)]. \quad (4)$$

Different forms of the function $f(q_1 + q_2)$ allow different types of correlations to be examined.

A. Assortative mixing

As a convenient example, we consider assortative correlations using a symmetric joint degree distribution

$$P(q_1, q_2, \tilde{q}) = \mathcal{P}(q_1, c) \mathcal{P}(q_2, c) \mathcal{P}[\tilde{q}, A(d + q_1 + q_2)]. \quad (5)$$

The parameter d controls the correlations, with $d \rightarrow 0$ corresponding to perfect assortativity, and $d \rightarrow \infty$ corresponding to the uncorrelated case. The coefficient A normalises the function to maintain the mean degree \tilde{c} required, $A = \tilde{c}/(d + 2c)$.

Replacing the distribution $P(q_1, q_2, \tilde{q})$ in Eqs. (2) with Eq. (5) we arrive at the system of equations:

$$\begin{aligned}
x &= 1 - 2 \exp\{-2c - A(1+d)(u+w) - c(x-2)e^{-A(u+w)}\} \\
&\quad + \exp\{-2c - A(1+d)(2u+w) - 2c(x-1)e^{-A(2u+w)}\}, \\
u &= \frac{1-w}{2} - \frac{A}{2\tilde{c}} \left\{ 2c(1-x) + de^{A(2u+w)} \right\} \\
&\quad \times \exp\{-2c - A(1+d)(2u+w) - 2c(x-1)e^{-A(2u+w)}\}, \\
w &= 1 - u - \frac{A}{\tilde{c}} \left\{ c(2-x) + de^{A(u+w)} \right\} \\
&\quad \times \exp\{-2c - A(1+d)(u+w) - c(x-2)e^{-A(u+w)}\}. \quad (6)
\end{aligned}$$

Then the expression for the relative size of the mutual component S is obtained by substituting Eq. (5) in Eqs. (2):

$$\begin{aligned}
S &= 1 - 2 \exp\{-2c - Ad(u+w) - c(x-2)e^{-A(u+w)}\} \\
&\quad + \exp\{-2c - Ad(2u+w) - 2c(x-1)e^{-A(2u+w)}\}. \quad (7)
\end{aligned}$$

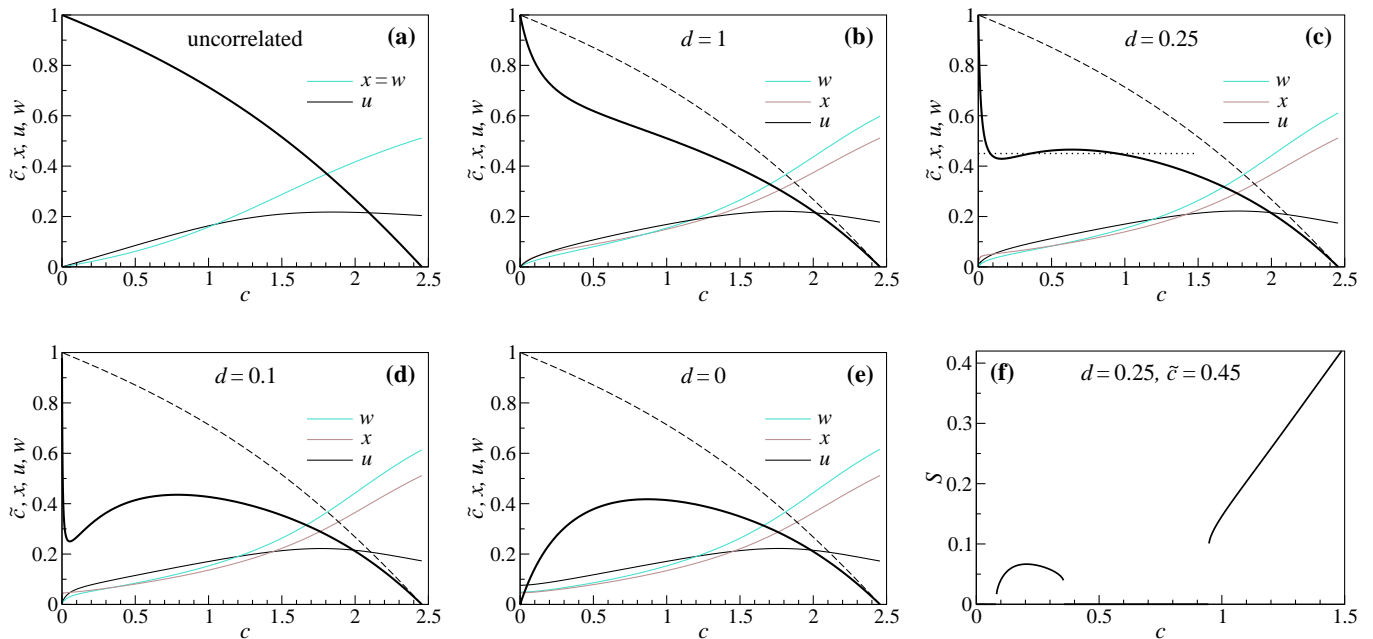


FIG. 2. (Color online) Phase diagrams in the \tilde{c} vs. c plane for the uncorrelated and assortatively correlated cases. The appearance of the giant mutually connected component with a discontinuous hybrid transition is shown as the heavy black line. (a) Symmetric uncorrelated joint degree distribution. (b)–(e) Assortative correlations of Eq. (5) for $d = 1, 0.25, 0.1,$ and 0 , respectively. For comparison, the dashed line shows the boundary between phases in the uncorrelated case. The plots also show the values of the probabilities $x = y, u = v,$ and w immediately above the discontinuous transition. (f) Multiple transitions of S for $d = 0.25$, fixed $\tilde{c} = 0.45$ and varying c , i.e. along the dotted line of panel (c).

Figure 2 shows phase diagrams for different values of the constant d . As the assortativity becomes stronger (d decreases) the giant mutual component appears at smaller values of \tilde{c} , except at the endpoints. The right-hand end point is at $(c, \tilde{c}) = (2.4554\dots, 0)$ (in agreement with the critical point without overlaps found in [9]).

As d approaches 0 the critical line approaches that found for $d = 0$ (panel (e)), however the left-hand end point remains at $(c, \tilde{c}) = (0, 1)$ for all $d > 0$, and jumps to $(0, 0)$ at $d = 0$. For small d the phase boundary is non-monotonic with respect to c , meaning that multiple hybrid transitions may be encountered when following a straight trajectory across the phase plane, as demonstrated in panel (f), which shows the variation of the size S of the mutual component along the dotted line in panel (c). Notice the recurrent hybrid transition after which S returns to zero.

Multiple hybrid transitions have not previously been observed in this type of system, although multiple transitions have been noted in networks of networks [10] and several other network percolation problems [11–15].

B. Disassortative mixing

An example of a symmetric joint degree distribution with disassortative correlations is

$$P(q_1, q_2, \tilde{q}) = \mathcal{P}(q_1, c) \mathcal{P}(q_2, c) \mathcal{P}[\tilde{q}, A(q_{\text{cut}} - q_1 - q_2)]. \quad (8)$$

Larger values of q_{cut} correspond to weaker correlations, with the anticorrelations becoming stronger as q_{cut} decreases. Once again, the value of A must be chosen to maintain the required value of $\tilde{c} = \sum_{q_1, q_2, \tilde{q}} \tilde{q} P(q_1, q_2, \tilde{q})$,

$$A = \frac{\tilde{c} [q_{\text{cut}}]!}{(2c)^{1+[q_{\text{cut}}]} e^{-2c} + (q_{\text{cut}} - 2c) \Gamma([q_{\text{cut}}] + 1, 2c)}, \quad (9)$$

where $[q_{\text{cut}}]$ is the largest integer smaller or equal to q_{cut} .

Again using a Poisson distribution for $\mathcal{P}(q, c)$ with first moment c , and inserting Eq. (8) in Eq. (2) leads to the following system of three transcendental equations:

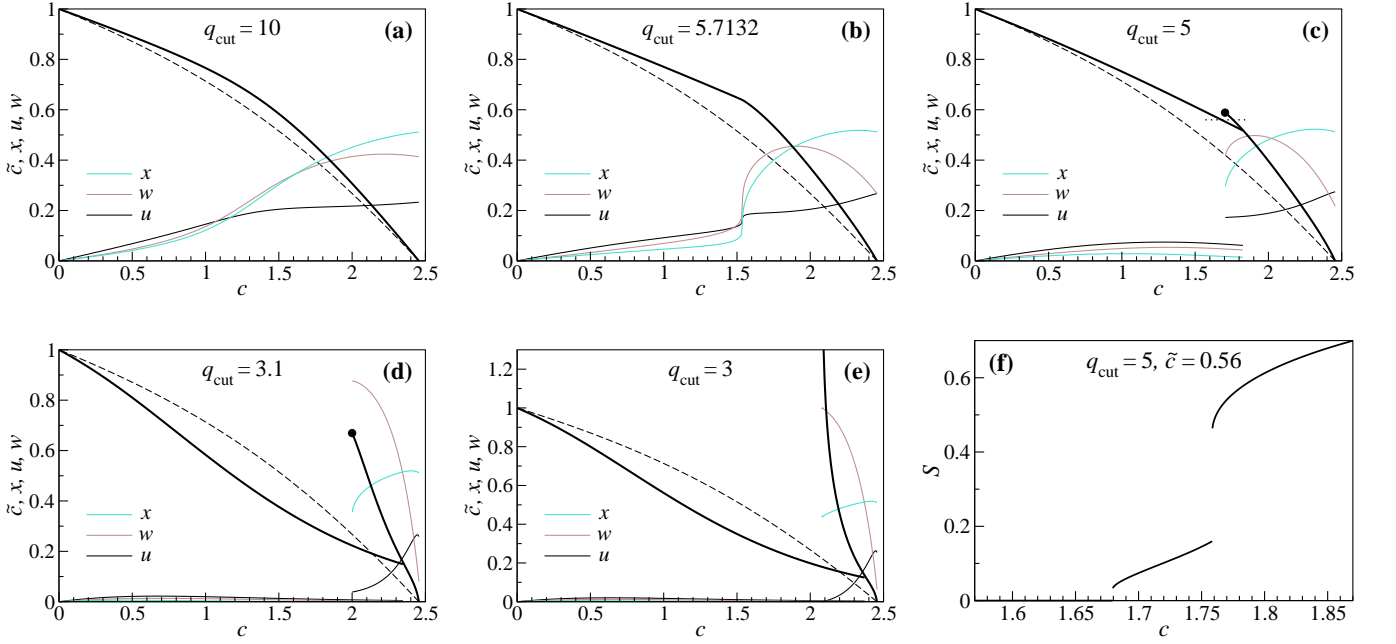


FIG. 3. (Color online) Phase diagrams in the \tilde{c} vs. c plane for the disassortatively correlated case defined by Eq. (8). The appearance of the giant mutually connected component with a discontinuous hybrid transition is shown as the heavy black line. (a)–(e) Disassortative correlations of Eq. (8) for $q_{\text{cut}} = 10, 5.7132, 5.5, 5,$ and 3 . For $q_{\text{cut}} < 5.7131\dots$ instead of a single line of transitions there are two branches, and for $q_{\text{cut}} < 3$ the right-hand side branch extends to $\tilde{c} = \infty$. The dashed line is the phase boundary in the uncorrelated case. The plots also show the values of the probabilities immediately above the discontinuous transition. (f) Multiple transitions of S for $q_{\text{cut}} = 5$, fixed $\tilde{c} = 0.56$ and c varying along the dotted line of panel (c).

$$\begin{aligned}
 x &= \frac{e^{-2\tilde{c}}}{\Gamma(\lfloor q_{\text{cut}} \rfloor)} \left\{ e^{2\tilde{c}(1-x)} (e^{\tilde{c}x} - 1)^2 \Gamma(\lfloor q_{\text{cut}} \rfloor) + 2e^{\tilde{c}(2-x)} \Gamma(\lfloor q_{\text{cut}} \rfloor, \tilde{c}(2-x)) - e^{2\tilde{c}(1-x)} \Gamma(\lfloor q_{\text{cut}} \rfloor, 2\tilde{c}(1-x)) \right. \\
 &\quad \left. + \exp \left[-A(q_{\text{cut}} - 1)(2u + w) + 2\tilde{c}(1-x)e^{A(2u+w)} \right] \Gamma(\lfloor q_{\text{cut}} \rfloor, 2\tilde{c}(1-x)e^{A(2u+w)}) \right. \\
 &\quad \left. - 2 \exp \left[-A(q_{\text{cut}} - 1)(u + w) + \tilde{c}(2-x)e^{A(u+w)} \right] \Gamma(\lfloor q_{\text{cut}} \rfloor, \tilde{c}(2-x)e^{A(u+w)}) \right\}, \\
 u &= \frac{1-w}{2} + \frac{A \exp \left[-Aq_{\text{cut}}(2u+w) - 2\tilde{c}(1-x)e^{A(2u+w)} \right]}{2\tilde{c}\Gamma(\lfloor q_{\text{cut}} \rfloor + 1)} \left\{ 2\tilde{c}e^{A(2u+w)} \lfloor q_{\text{cut}} \rfloor (1-x) \Gamma(\lfloor q_{\text{cut}} \rfloor, 2\tilde{c}(1-x)e^{A(2u+w)}) \right. \\
 &\quad \left. - q_{\text{cut}} \Gamma(\lfloor q_{\text{cut}} \rfloor + 1, 2\tilde{c}(1-x)e^{A(2u+w)}) \right\}, \\
 w &= 1 - u + \frac{A \exp \left[-Aq_{\text{cut}}(u+w) - \tilde{c}(2-x)e^{A(u+w)} \right]}{2\tilde{c}\Gamma(\lfloor q_{\text{cut}} \rfloor + 1)} \left\{ \tilde{c}e^{A(u+w)} \lfloor q_{\text{cut}} \rfloor (2-x) \Gamma(\lfloor q_{\text{cut}} \rfloor, \tilde{c}(2-x)e^{A(u+w)}) \right. \\
 &\quad \left. - q_{\text{cut}} \Gamma(\lfloor q_{\text{cut}} \rfloor + 1, \tilde{c}(2-x)e^{A(u+w)}) \right\}. \tag{10}
 \end{aligned}$$

The expression for the mutual component size S in a network with these correlations is obtained substituting Eq. (8) for $P(q_1, q_2, \tilde{q})$ in Eq. (2):

$$\begin{aligned}
 S &= \frac{e^{-2\tilde{c}}}{\Gamma(\lfloor q_{\text{cut}} \rfloor + 1)} \left\{ e^{2\tilde{c}(1-x)} (e^{\tilde{c}x} - 1)^2 \Gamma(\lfloor q_{\text{cut}} \rfloor + 1) + 2e^{\tilde{c}(2-x)} \Gamma(\lfloor q_{\text{cut}} \rfloor + 1, \tilde{c}(2-x)) - e^{2\tilde{c}(1-x)} \Gamma(\lfloor q_{\text{cut}} \rfloor + 1, 2\tilde{c}(1-x)) \right. \\
 &\quad \left. + \exp \left[-Aq_{\text{cut}}(2u+w) + 2\tilde{c}(1-x)e^{A(2u+w)} \right] \Gamma(\lfloor q_{\text{cut}} \rfloor + 1, 2\tilde{c}(1-x)e^{A(2u+w)}) \right. \\
 &\quad \left. - 2 \exp \left[-Aq_{\text{cut}}(u+w) + \tilde{c}(2-x)e^{A(u+w)} \right] \Gamma(\lfloor q_{\text{cut}} \rfloor + 1, \tilde{c}(2-x)e^{A(u+w)}) \right\}. \tag{11}
 \end{aligned}$$

Solving these equations, we find a more complex phase diagram than in the positively correlated case. Phase

diagrams for different values of q_{cut} are shown in Fig. 3.

For weak anticorrelations, with q_{cut} larger than a specific value $q_{\text{cut}}^* = 5.7131\dots$, panels (a) and (b), the phase diagram is qualitatively similar to the uncorrelated case, containing a single line of discontinuous phase transitions with end points $(c, \tilde{c}) = (0, 1)$ and $(2.4554\dots, 0)$, compare to Fig. 2(a). The line of transition moves toward larger values of \tilde{c} , while the endpoints again remain fixed. At $q_{\text{cut}} = q_{\text{cut}}^*$ a new behavior emerges, as the line of continuous transitions breaks into two branches having different values of S above the transition. For $q_{\text{cut}} < q_{\text{cut}}^*$ the lower branch that starts at $(0, 1)$ finishes when it meets the other branch. The branch that starts at $(2.4554\dots, 0)$ ends at a finite point for $3 < q_{\text{cut}} < q_{\text{cut}}^*$, panels (c) and (d), but extends to $\tilde{c} = \infty$ for $q_{\text{cut}} \leq 3$, panel (e). An example of the solution of these equations is shown in panel (f) of Fig. 3. This panel shows the size of the mutual component S along the dotted line in panel (c), compare with the assortative case, Fig. 2(f).

The disassortative correlations partially separate the nodes into two populations: one of nodes with a majority of single connections, and another with a majority of overlapped connections. This is reflected in the relative order of the probabilities x , w , and u in panels (b)–(e) of Fig. 3. In the first branch, u (which incorporates effects of overlapped edges) dominates, followed by w then x , whereas in the second branch, u makes the smallest contribution. In the example shown in panel (f) the first jump occurs when a giant mutual component is first formed, with nodes containing both single and overlapping edges. Nodes with more than q_{cut} single edges have no overlapped edges. The second jump occurs when a large number of such nodes are recruited to the giant component. By comparison, in the uncorrelated and assortative cases, there is no such separation of node populations.

We also consider an alternative form for the disassortative correlations, where the cut-off degree varies linearly with the average number of single edges $q_{\text{cut}} = Bc$,

$$P(q_1, q_2, \tilde{q}) = \mathcal{P}(q_1, c)\mathcal{P}(q_2, c)\mathcal{P}[\tilde{q}, A(Bc - q_1 - q_2)], \quad (12)$$

for different values of B . Here the constant A is determined by Eq. (9) with Bc substituted for q_{cut} . Similarly, the self-consistency equations and the expression for S are obtained by substituting Bc for q_{cut} in Eqs. (10) and (11), respectively.

Figure 4 shows the solution of the model $q_{\text{cut}} = Bc$ for different B , which is qualitatively similar to the one of the model with constant q_{cut} . We again find a single line of discontinuous hybrid transitions for weak anticorrelations, panels (a) and (b). As before, at a specific strength of the anticorrelations, $B = 3.7165\dots$, the line of transition breaks into two branches. Below this value of B , panels (c) and (d), we find two branches of transitions, with the end point of the second branch diverging to $\tilde{c} = \infty$ for $B < 1.497\dots$, panel (e). The different form of the degree correlation function gives a phase boundary with a more complex shape. A straight path in the phase

plane may cross this line multiple times, giving multiple hybrid transitions. An example is shown in panel (f), which shows the size of the mutual component S along the dotted line in panel (c). The size S jumps each time a line of discontinuous transitions is crossed.

As an effect of the correlations of Eq. (12), when $c \leq 1/B$ only nodes without single edges (i.e. $q_1 + q_2 = 0$) can have overlapping edges, which results in two disjoint subgraphs. On one hand, the subgraph containing all the single edges has a relative size $1 - e^{-2c}$, and does not contain a mutual component for $c < 2.4554\dots$. On the other hand, the subgraph consisting of the remaining nodes contains all the overlapping edges and has a relative size e^{-2c} . As a result, in the region $c \leq 1/B$ the overlapped subgraph behaves as a single-layer classical random graph, and undergoes a standard continuous transition at the dot-dashed line in Fig. 4. The continuous transition takes place when the average degree in the overlapped subgraph equals 1, that is, when $\tilde{c}/e^{-2c} = 1$.

V. NUMERICAL SIMULATIONS

In this section we present experimental results obtained from simulations of two-layered systems. In the first stage, we generate networks with the desired properties, namely a given average degree of each type of single edges, c , and the particular function $f(x)$ on the correlated joint degree distribution of Eq. (4). Recall that the $f(q_1 + q_2)$ is the average number of overlapping edges of nodes with q_1 edges of type 1 and q_2 edges of type 2. For a network with N nodes, we first place cN single links of each type connecting pairs of nodes chosen uniformly at random. Finally, we distribute $\tilde{c}N$ overlapping edges, by choosing pairs of nodes where each node gets picked independently with probability proportional to $f(q_1 + q_2)$.

We find the giant mutual component of the resulting network by iteratively following these steps:

(i) We find the largest cluster in each layer, and remove all nodes not belonging simultaneously to the largest cluster in both layers and all edges connected to the removed nodes. (Of course, in this stage of the algorithm, an overlapping edge is treated as two independent single edges.)

(ii) If the remaining subset of nodes and edges is the same size as before executing step (i), i.e., nothing was removed, then it is the giant mutual component. Otherwise, we return to step (i), but only with the remaining of the system.

This algorithm stops when all of the remaining nodes are in the same cluster in both layers, which means every node in this cluster can reach every other by paths strictly inside the cluster. This subset of nodes and edges forms the mutually connected cluster.

We performed simulations according to this prescription for systems of size $N = 10^5, 10^6, 10^7$, and 10^8 for each of the three example cases described in Sect. IV. For each value of c we generated a network of a given size and calculated the size of the largest cluster, according

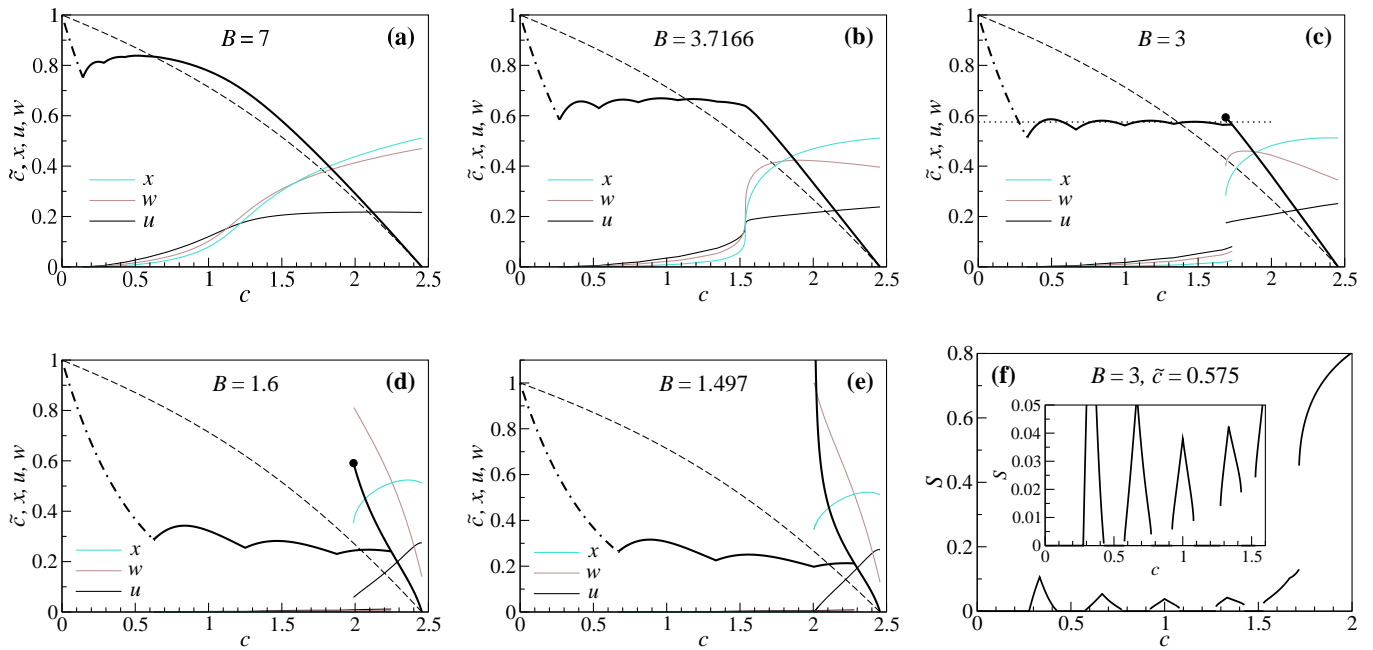


FIG. 4. (Color online) Phase diagrams in the \tilde{c} vs. c plane for the disassortatively correlated case defined by Eq. (12). The appearance of the giant mutually connected component with a discontinuous hybrid transition is shown as the heavy black line. (a)-(e) Disassortative correlations of Eq. (8) with $q_{\text{cut}} = Bc$, for $B = 7, 3.7166, 3.5, 1.6,$ and 1.497 . For $B < 3.7165\dots$ instead of a single line of transitions there are two branches, and for $B < 1.497\dots$ the right-hand side branch extends to $\tilde{c} = \infty$. The dot-dashed curve is a line of continuous phase transitions that take place at e^{-2c} for $c < 1/B$. The dashed line is the phase boundary in the uncorrelated case. The plots also show the values of the probabilities immediately above the discontinuous transition. (f) Multiple transitions of S for $B = 3$, fixed $\tilde{c} = 0.575$ and c varying along the dotted line of panel (c).

to the method described above. The results of the simulations are presented in Fig. 5, and show an excellent agreement with our theoretical predictions. Fluctuations reduce with system size, and are only significant for the case $N = 10^5$.

VI. CONCLUSIONS

In this Paper we have developed a theory for locally tree-like multiplex networks with overlapped edges allowing the giant mutual component in these networks to be found. The simplicity of our theory enables the study of more difficult and rich cases than previously possible. In particular this method allows for arbitrary inter-layer degree correlations and correlations in overlapped and single edge degrees. These correlations qualitatively change the phase diagrams for multiplex networks. We found qualitatively new features: new phase diagrams with multiple and recursive hybrid phase transitions. We observed the new phase diagrams for a particular form of the correlation function. To confirm our observations, we also considered a different form of correlations than in

Eq. (8) and arrived at similar results (see Supplementary Material). This allows us to suggest that our qualitative findings are valid for a wide range of correlations. Our method follows logically from the structure of the problem, writing an equation for each possible way to encounter the giant mutual component. Further generalisations, such as addition of more layers, should be able to be treated using the same logic, requiring more equations but not new techniques. Indeed since this paper was first submitted, such a generalization has already been proposed [16]. Previous methods do not have this advantage. Overlapping layers are an unavoidable feature of interdependent networks, naturally emerging in various problems [17], yet they make theoretical treatment much more difficult. We suggest that the simplicity and tractability of our theory and results will make this task much easier.

ACKNOWLEDGMENTS

This work was partially supported by the FET proactive IP project MULTIPLEX 317532. GJB was supported by the FCT grant No. SFRH/BPD/74040/2010.

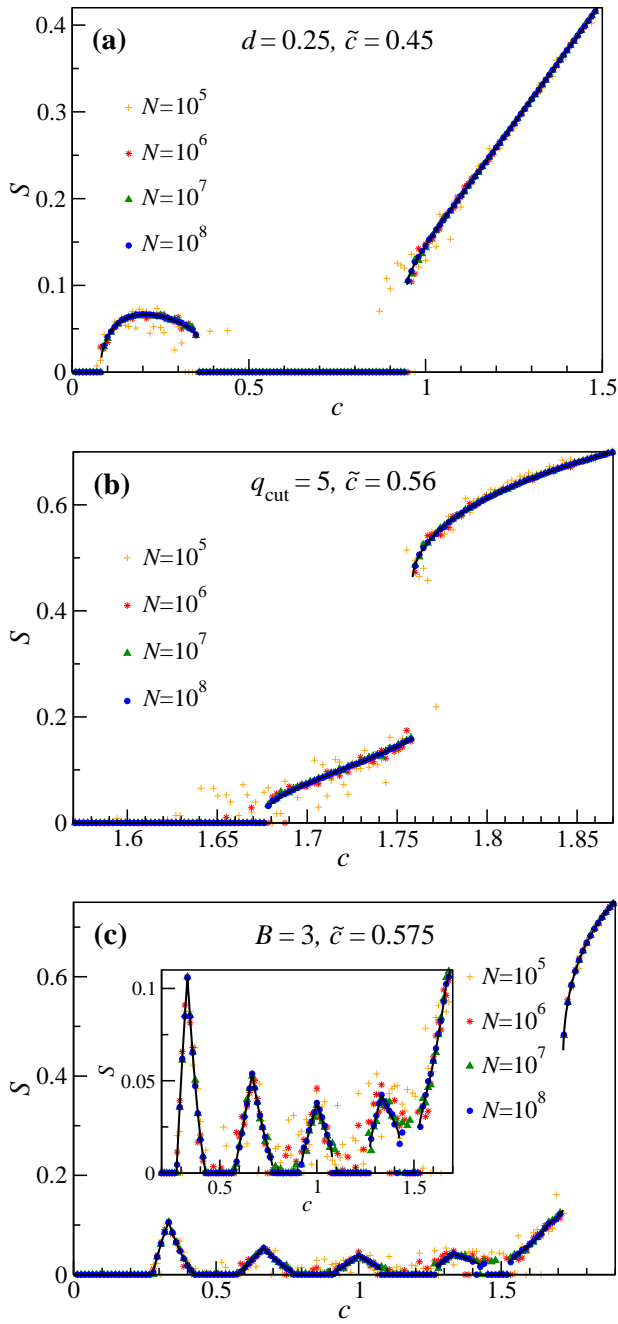


FIG. 5. (Color online) Size of the largest mutually connected component S as a function of mean non-overlapped degree c for correlated two layer multiplex with degree distribution of the form Eq. (4). Each point corresponds to a single network realisation of size $N = 10^5$ (orange pluses), 10^6 (red diamonds), 10^7 (green triangles), or 10^8 (blue circles). (a) Assortative correlations between overlapped and non-overlapped degree of the form Eq. (5). (b) Disassortative correlations as in Eq. (8). (c) Disassortative correlations as in Eq. (12). Theoretical results are also plotted (continuous black line), compare Figs. 2(f), 3(f), and 4(f), which show theoretical results for the same parameter choices.

-
- [1] S. Boccaletti, G. Bianconi, R. Criado, C. I. Del Genio, J. Gómez-Gardeñes, M. Romance, I. Sendina-Nadal, Z. Wang, and M. Zanin, *Phys. Reports* **544**, 1 (2014).
- [2] M. Kivelä, A. Arenas, M. Barthelemy, J. P. Gleeson, Y. Moreno, and M. A. Porter, *J. Complex Networks* **2**, 203 (2014).
- [3] S.-W. Son, G. Bizhani, C. Christensen, P. Grassberger, and M. Paczuski, *EPL* **97**, 16006 (2012).
- [4] G. J. Baxter, S. N. Dorogovtsev, A. V. Goltsev, and J. F. F. Mendes, *Phys. Rev. Lett.* **109**, 248701 (2012).
- [5] D. Cellai, E. López, J. Zhou, J. P. Gleeson, and G. Bianconi, *Phys. Rev. E* **88**, 052811 (2013).
- [6] Y. Hu, D. Zhou, R. Zhang, Z. Han, C. Rozenblat, and S. Havlin, *Phys. Rev. E* **88**, 052805 (2013).
- [7] B. Min, S. Lee, K.-M. Lee, and K.-I. Goh, *Chaos, Solitons & Fractals* **72**, 49 (2015).
- [8] G. Bianconi, *Phys. Rev. E* **87**, 062806 (2013).
- [9] S. V. Buldyrev, R. Parshani, R. Paul, H. E. Stanley, and S. Havlin, *Nature* **464**, 1025 (2010).
- [10] G. Bianconi and S. N. Dorogovtsev, *Phys. Rev. E* **89**, 062814 (2014).
- [11] J. Nagler, T. Tiessen, and H. W. Gutch, *Physical Review X* **2**, 031009 (2012).
- [12] W. Chen, J. Nagler, X. Cheng, X. Jin, H. Shen, Z. Zheng, and R. M. DSouza, *Physical Review E* **87**, 052130 (2013).
- [13] W. Chen, X. Cheng, Z. Zheng, N. N. Chung, R. M. D'Souza, and J. Nagler, *Physical Review E* **88**, 042152 (2013).
- [14] P. Colomer-de Simón and M. Boguñá, *Physical Review X* **4**, 041020 (2014).
- [15] A. Hackett, D. Cellai, S. Gómez, A. Arenas, and J. P. Gleeson, *Phys. Rev. X* **6**, 021002 (2016).
- [16] D. Cellai, S. N. Dorogovtsev, and G. Bianconi, *arXiv:1604.05175* (2016).
- [17] N. Azimi-Tafreshi, *arXiv:1511.03235* (2015).

Appendix: Extended form of Main Equations

To aid the reader, we give here forms of the equations for x, y, u, v , and w with terms corresponding to each term of the diagrammatic equations Fig. 1. Simplification of these equations leads to Eqs. (2).

$$\begin{aligned}
x &= \sum_{q_1, q_2, \tilde{q}} \frac{q_1}{\langle q_1 \rangle} P(q_1, q_2, \tilde{q}) \left\{ [1 - (1-x)^{q_1-1}] [1 - (1-y)^{q_2}] (1-u-v-w)^{\tilde{q}} \right. \\
&\quad + [1 - (1-x)^{q_1-1}] [(1-u-w)^{\tilde{q}} - (1-u-v-w)^{\tilde{q}}] + [1 - (1-y)^{q_2}] [(1-v-w)^{\tilde{q}} - (1-u-v-w)^{\tilde{q}}] \\
&\quad \left. + [(1-w)^{\tilde{q}} - (1-w-u)^{\tilde{q}} - (1-w-v)^{\tilde{q}} + (1-w-u-v)^{\tilde{q}}] + [1 - (1-w)^{\tilde{q}}] \right\}, \\
y &= \sum_{q_1, q_2, \tilde{q}} \frac{q_2}{\langle q_2 \rangle} P(q_1, q_2, \tilde{q}) \left\{ [1 - (1-x)^{q_1}] [1 - (1-y)^{q_2-1}] (1-u-v-w)^{\tilde{q}} \right. \\
&\quad + [1 - (1-x)^{q_1}] [(1-u-w)^{\tilde{q}} - (1-u-v-w)^{\tilde{q}}] + [1 - (1-y)^{q_2-1}] [(1-v-w)^{\tilde{q}} - (1-u-v-w)^{\tilde{q}}] \\
&\quad \left. + [(1-w)^{\tilde{q}} - (1-u-w)^{\tilde{q}} - (1-v-w)^{\tilde{q}} + (1-u-v-w)^{\tilde{q}}] + [1 - (1-w)^{\tilde{q}}] \right\}, \\
u &= \sum_{q_1, q_2, \tilde{q}} \frac{\tilde{q}}{\langle \tilde{q} \rangle} P(q_1, q_2, \tilde{q}) \left\{ [1 - (1-x)^{q_1}] (1-y)^{q_2} (1-u-v-w)^{\tilde{q}-1} + (1-y)^{q_2} [(1-v-w)^{\tilde{q}-1} - (1-u-v-w)^{\tilde{q}-1}] \right\}, \\
v &= \sum_{q_1, q_2, \tilde{q}} \frac{\tilde{q}}{\langle \tilde{q} \rangle} P(q_1, q_2, \tilde{q}) \left\{ (1-x)^{q_1} [1 - (1-y)^{q_2}] (1-u-v-w)^{\tilde{q}-1} + (1-x)^{q_1} [(1-u-w)^{\tilde{q}-1} - (1-u-v-w)^{\tilde{q}-1}] \right\}, \\
w &= \sum_{q_1, q_2, \tilde{q}} \frac{\tilde{q}}{\langle \tilde{q} \rangle} P(q_1, q_2, \tilde{q}) \left\{ [1 - (1-x)^{q_1}] [1 - (1-y)^{q_2}] (1-u-v-w)^{\tilde{q}-1} \right. \\
&\quad + [1 - (1-y)^{q_2}] [(1-v-w)^{\tilde{q}-1} - (1-v-w-u)^{\tilde{q}-1}] + [1 - (1-x)^{q_1}] [(1-u-w)^{\tilde{q}-1} - (1-v-w-u)^{\tilde{q}-1}] \\
&\quad \left. + [(1-w)^{\tilde{q}-1} - (1-w-u)^{\tilde{q}-1} - (1-w-v)^{\tilde{q}-1} + (1-w-u-v)^{\tilde{q}-1}] + [1 - (1-w)^{\tilde{q}-1}] \right\}. \tag{A.1}
\end{aligned}$$
